Fabrication and Characterization of Anodic Titanium Oxide Nanotube Arrays of Controlled Length for Highly Efficient Dye-Sensitized Solar Cells

Chien-Chon Chen,[†] Hsien-Wen Chung,[†] Chin-Hsing Chen,[†] Hsueh-Pei Lu,[†] Chi-Ming Lan,[†] Si-Fan Chen,[†] Liyang Luo,[†,‡] Chen-Shiung Hung,[‡] and Eric Wei-Guang Diau*[,†]

Department of Applied Chemistry and Institute of Molecular Science, National Chiao Tung University, No. 1001, Ta Hsueh Road, Hsinchu 300, Taiwan, and and Institute of Chemistry, Academia Sinica, Taipei 115, Taiwan

Received: July 16, 2008; Revised Manuscript Received: September 2, 2008

The performance of dye-sensitized solar cells (DSSC), made of highly ordered anodic titanium oxide (ATO) nanotube (NT) arrays produced directly on Ti foil, depends on the length of these arrays. We controlled these lengths L from 4 to 41 μm while varying the concentration (0.1, 0.25, 0.5, and 0.8 wt %) of the electrolyte (NH_4F) in ethylene glycol in the presence of H_2O (2 vol %) with anodization for various periods ($t = 0.5-8$ h). The compact and bundle layers introduced during anodization were effectively removed upon simple ultrasonic cleaning in deionized water containing submicrometer particles of Al_2O_3 in a small proportion. The photovoltaic performance of the NT-DSSC devices (NH_4F at 0.5 wt %) made of ATO films, as prepared, increased from 3.0% to 5.2% as L was increased from 6 μm ($t = 0.5$ h) to 30 μm ($t = 8$ h). After treatment of the ATO films with $TiCl_4$ in a two-step annealing process, the optimized NT-DSSC device attained an overall efficiency of 7.0% power conversion.

1. Introduction

Following the pioneering work of Grätzel and co-workers,[1] dye-sensitized solar cells (DSSC) have received much attention as an economical energy conversion device. A typical DSSC device contains a light-harvesting layer on a working electrode (anode) and a Pt-coated layer on a counter electrode (cathode); both electrodes are made of a transparent conducting oxide (TCO) substrate; an iodine-based electrolyte fills the space between the anode and the cathode to serve as a redox mediator in a sandwich-type structure. As a light-harvesting layer, a photosensitizer, typically a ruthenium complex such as N3 or N719 dye, is chemisorbed onto the surface of a nanocrystalline thin film of TiO_2. When this photosensitizer absorbs sunlight, electrons are injected into the conduction band of the semiconductor layer, which results in a separation of electrons (in the TiO_2 layer) and holes (dye cations); the electrons proceed to the anode while the holes are transported by the redox species to the cathode to complete the photoelectrochemical cycle and to do external work. The electron-collecting layer (anode) of a DSSC is traditionally composed of randomly packed TiO_2 nanoparticles (NP). With sunlight irradiating the transparent anode (front illumination), the greatest efficiency (η) of conversion into photovoltaic power of a NP-DSSC device has reached $\sim$11%.[2–6]

A great advantage of a NP-DSSC is that nanoporous TiO_2 films have a large surface area for dye adsorption, but diffusion, limited by traps, for electron transport in NP-DSSC impedes the efficiency of conversion of light to electricity.[7,8] To improve the efficiency of charge collection by promoting both more rapid electron transport and slower charge recombination, several methods with TiO_2 films constructed of oriented one-dimensional (1D) nanostructures have been established. For instance, DSSC based on one-dimensional TiO_2 nanowires have been reported;[9,10] 1D TiO_2 nanotubes (NT) have been synthesized using the sol−gel method[11–13] and potentiostatic anodization.[8,14–20]

Grätzel and co-workers reported a back-illuminated NP-DSSC with a cell performance $\eta = 7.2\%$.[21] Because substantial light scattering at the Pt-coated counter electrode and light absorption by the iodine-based electrolyte adversely affect the performance, the back-illuminated NP-DSSC has an efficiency significantly smaller than that of its front-illuminated counterpart ($\eta = 9.9\%$); maximum values occur at a TiO_2 film thickness of 14 μm in both cases.[21] For NT-DSSC, perpendicularly aligned and highly ordered anodic titanium oxide (ATO) NT arrays are prepared either on a TCO glass, using combined sputtering/anodization[8] or a film detachment,[20] or on a nontransparent Ti metal surface, using direct anodization.[14–19] Front illumination is feasible for only the former case, but poor adhesion between the ATO barrier layer and the TCO layer limits the length of ATO NT arrays.

Although illumination from the back suffers from the specified disadvantages, NT-DSSC with ATO NT arrays on Ti foil as working electrodes have many important intrinsic features that outperform conventional NP-DSSC. First, the efficiency of charge collection of NT films has been proved to be much better than that of NP films because of the 1D nature of the former with a much smaller rate of charge recombination;[16] this intrinsic advantage of NT-DSSC significantly promotes its cell performance with increasing tube length up to 20 μm as reported by Grimes and co-workers.[17] Second, the efficiency of light harvesting by NT films is much better than that of NP films because the former have a stronger light scattering effect;[16] for a traditional, highly efficient NP-DSSC, adding an additional TiO_2 layer of larger particles (size $\sim$400 nm)[2,3,21] or increasing the haze factor[5,6] was required to increase the light scattering, whereas this effect is a natural property of a NT-DSSC. Third, the anode fabrication of a NT-DSSC is much simpler and cheaper than that of a NP-DSSC. Direct anodization of a Ti

* Corresponding author. Fax: (886)-03-572-3764. E-mail: diau@mail.nctu.edu.tw.
[†] National Chiao Tung University.
[‡] Academia Sinica.

10.1021/jp806281r CCC: $40.75
Published on Web 11/08/2008

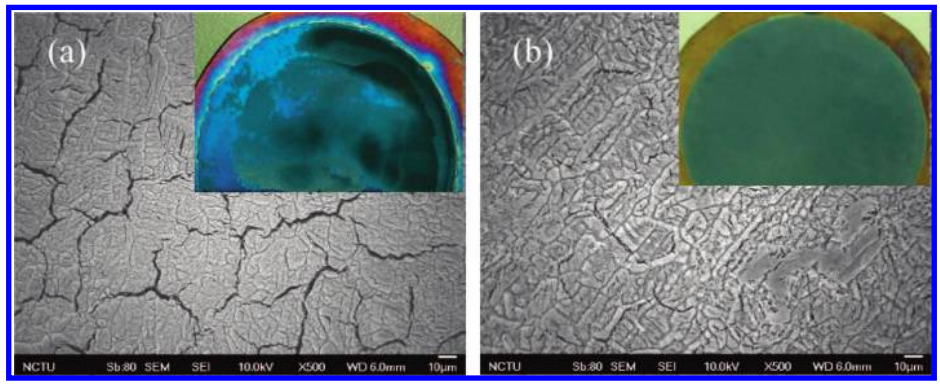

Figure 1. SEM images of ATO films undergoing (a) a one-step annealing and (b) a two-step annealing. The insets show specimen pictures of the corresponding ATO films: the one-step process leads to creaking of the films that easily peeled from the Ti substrate, whereas the two-step process yields films of satisfactory quality and ready to use.

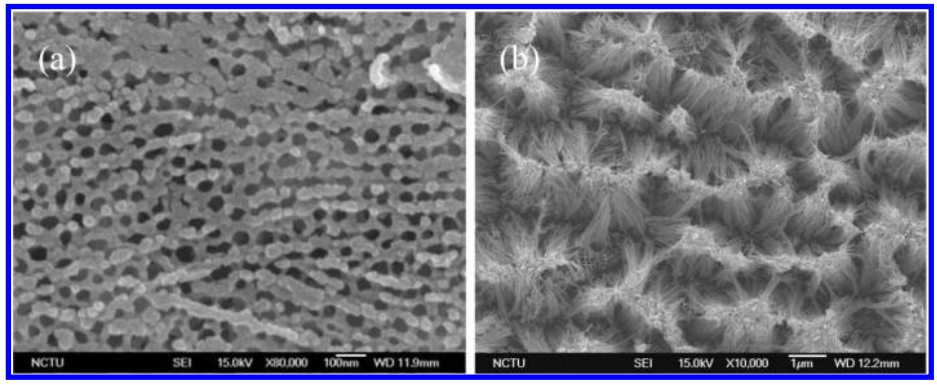

Figure 2. SEM images of ATO NT covered with (a) a compact layer and (b) a bundle layer before ultrasonic cleaning.

foil in one step produces a blank TiO_2 film ready to act as a working electrode for a NT-DSSC, whereas making a blank TiO_2 film for a NP-DSSC requires multiple coatings—at least two layers of TiO_2 NP coating on an expensive TCO substrate. Furthermore, calcination of the NT/Ti anode at a high temperature makes it ready to be fabricated into a flexible NT-DSSC device with a transparent conductive plastic cathode (ITO/PEN). Grätzel and co-workers reported an efficiency of 3.6% photovoltaic conversion for a flexible NT-DSSC made of ATO NT films of thickness 14 μm with a solvent-free ionic liquid electrolyte.[19]

Even though the TiO_2 NT arrays possess the advantages of greater efficiency of charge collection and stronger light scattering than their NP-based counterparts,[16] producing longer tubes on a larger area involves formation of a bundle layer in the films, leading to cracking of films that are easily peeled from the Ti substrate. To resolve this problem, Frank and co-workers[22] removed solvent liquids from the mesopores of the arrays with supercritical CO_2, so producing NT films free of bundles and cracks for NT-DSSC applications, but the small length of the TiO_2 NT arrays ($L = 6.1$ μm) limited the efficiency of power conversion of the device ($\eta = 1.9\%$).[22] The greatest reported efficiency of NT-DSSC under backside illumination is 6.89%.[17]

In the present work, we controlled the lengths of ATO NT from 4 to 41 μm while varying the concentration of NH_4F electrolyte in ethylene glycol (EG) with anodization for various periods. The unwanted surface deposits of the films introduced during anodization were effectively removed simply upon ultrasonic cleaning in deionized water containing Al_2O_3 as submicrometer particles in a small proportion. We observed a systematic variation of the photovoltaic performance of the NT-DSSC devices as a function of tube length. After the ATO films were treated with $TiCl_4$ and annealed in two steps, we found that, with an appropriate redox electrolyte and an improved counter electrode, the optimized NT-DSSC device reaches an overall efficiency of 7.0% power conversion.

2. Experimental Section

We fabricated ordered nanochannel arrays of ATO films at 25 °C on anodizing titanium (Ti) foil (Aldrich, 99.7% purity) as circular discs (diameter ~50 mm) at a constant voltage of 60 V.[17,23] The electrolyte solutions contained ammonium fluoride (NH_4F, 99.9%; 0.15, 0.25, 0.5, and 0.8 wt %) in EG in the presence of H_2O (2 vol %, pH = 6.8) with anodization for varied periods ($t = 0.5-8$ h). To crystallize amorphous TiO_2 into its anatase phase, we annealed the samples to 450 °C. Parts a and b of Figure 1 show SEM images of the ATO films subjected to annealing in one and two steps, respectively. For the two-step process, the ATO films were first rinsed with ethanol, dried in air, and annealed at 150 °C for 2 h to remove organic solvents, and were then crystallized at 450 °C for another 3 h in an air furnace. After one-step annealing directly at 450 °C, the ATO film suffered severe cracking that resulted in the film becoming easily peeled from the Ti-foil substrate, as demonstrated in the inset of Figure 1a. The inset of Figure 1b shows the satisfactory quality of the ATO films of large area from the two-step annealing.

When the ATO NT were produced with the electrolyte at large concentrations or with protracted anodization, we observed the formation of compact layers on the surface of the ATO films (Figure 2a); a bundle layer was observed (Figure 2b) at a smaller anodization period, as Frank and co-workers reported.[22] Because of the robust structure of the NT arrays and the loose structure of the surface debris, the unwanted deposits on the ATO surface

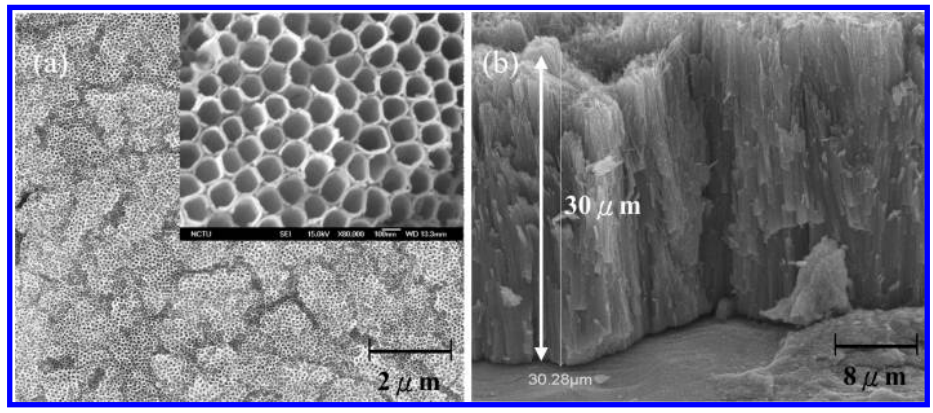

Figure 3. SEM images of ATO NT after ultrasonic cleaning: (a) top view and (b) side view. The inset of (a) shows the enlarged pattern of the ATO NT arrays.

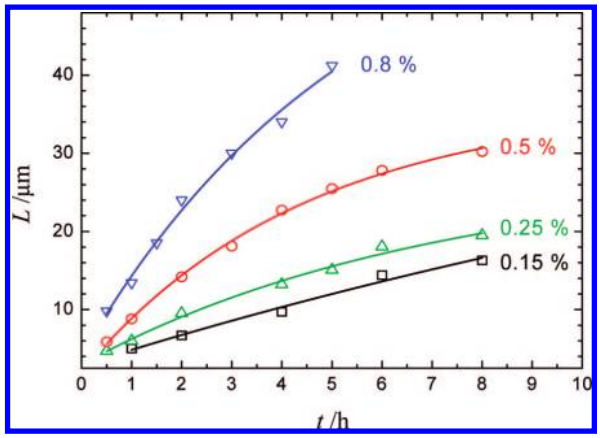

Figure 4. Length of ATO NT (L) as a function of anodization period (t) at various NH_4F concentrations (wt %) as indicated; the corresponding side-view SEM images showing the L values of each datum are given in the Supporting Information.

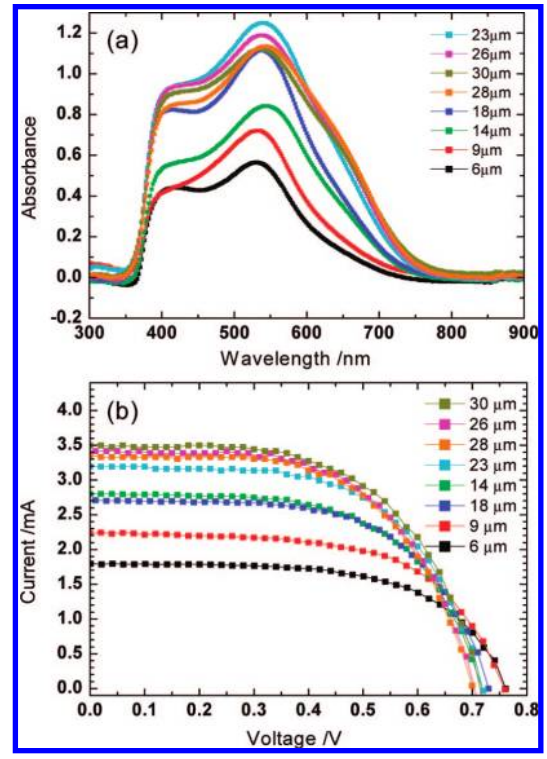

Figure 5. (a) Absorption spectra of ATO films sensitized with N3 dye at various tube lengths produced with NH_4F (0.5 wt %). (b) Current−voltage characteristics of NT-DSSC devices fabricated using the corresponding ATO films (a) under simulated AM-1.5 solar illumination (100 mW cm^{-2}) and active area 0.28 cm^2.

introduced during anodization can be effectively removed with ultrasonic vibration of the ATO films in deionized water containing a small proportion of Al_2O_3 particles of average size 300 nm. Parts a and b of Figure 3 show top and side views of SEM images of ATO films after ultrasonic cleaning that completely removed the disordered clumps, but the length of the tube decreased from 36 to 30 μm. Afterward, the samples were again washed with ethanol, dried in air, and heated to 100 °C for 10 min followed by annealing at 450 °C for 30 min.

The surface roughness of ATO films was measured with a surface profiler (α-step; KOSAKA, ET-4000); these films were characterized with parameters for average roughness (Ra), root-mean-square roughness (Rq), and average maximum height of the profile (Rz). For a typical ATO film, these roughness parameters before ultrasonic treatment were Ra = 0.46 μm, Rq = 0.53 μm, and Rz = 2.91 μm; the parameters after that treatment were Ra = 0.80 μm, Rq = 0.93 μm, and Rz = 4.38 μm. We therefore estimate the uncertainty of the ATO film thickness to be ±2 μm according to the measured 2Rq values (two standard errors). The morphology of the ATO films was determined with a scanning electron microscope (SEM; JEOL 6500) and the composition with X-ray diffraction (XRD; Philips X'Pert Pro).

To characterize the photovoltaic performance of the NT-DSSC devices, we immersed the ATO films (typical size 1.2 × 2.0 cm^2) in an ethanol solution containing N3 (0.5 mM, Solaronix, Switzerland) at 50 °C for 8 h to absorb sufficient N3 dye for light harvesting; the N3/ATO films served as a working electrode (anode). A fluorine-doped tin oxide (FTO; 30 Ω/sq, Sinonar, Taiwan) glass (typical size 1.0 × 2.0 cm^2) coated with Pt particles by sputtering served as a counter electrode (cathode). To fabricate the NT-DSSC device, we assembled the two electrodes into a cell of sandwich type and sealed it with a hot-melt film (SX1170, Solaronix, thickness 25 μm); a thin layer of electrolyte was introduced into the space between the two electrodes.[17,18] A typical redox electrolyte contained lithium iodide (LiI, 0.1 M), diiodine (I_2, 0.01 M), 4-*tert*-butylpyridine (TBP, 0.5 M), butyl methyl imidazolium iodide (BMII, 0.6 M), and guanidinium thiocyanate (GuNCS, 0.1 M) in a mixture of acetonitrile (CH_3CN, 99.9%) and valeronitrile (n-C_4H_9CN, 99.9%) (v/v = 15/1).

The amount of N3 dye absorbed on the ATO films was measured with a UV−visible−NIR spectrophotometer (JASCO V-570) equipped with an integrating sphere (JASCO ISN-470). Measurements of IV curves were made with a digital source meter (Keithley 2400, computer-controlled) with the device

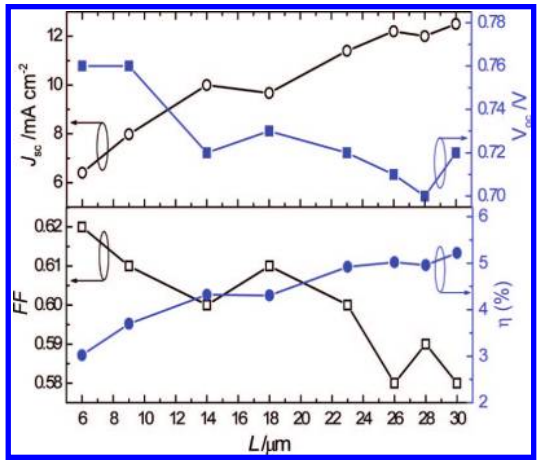

Figure 6. Variation of photovoltaic parameters J_{SC}, V_{OC}, FF, and η, as a function of tube length (L); these data were obtained from analysis of *IV* curves in Figure 5b and summarized in Table 1.

TABLE 1: Photovoltaic Performance of NT DSSC as a Function of Tube Length (L) under AM-1.5 Illumination (Power 100 mW cm^{-2}) and Active Area 0.28 cm^2[a]

t/h	L/μm	J_{SC}/mA cm^{-2}	V_{OC}/V	FF	η/%
0.5	6	6.4	0.76	0.62	3.0
1	9	8.0	0.76	0.61	3.7
2	14	10.0	0.72	0.60	4.3
3	18	9.7	0.73	0.61	4.3
4	23	11.4	0.72	0.60	4.9
5	26	12.2	0.71	0.58	5.0
6	28	12.0	0.70	0.59	5.0
8	30	12.5	0.72	0.58	5.2

[a] Values obtained for ATO films without $TiCl_4$ treatment; the counter electrodes were not optimized.

under one-solar AM-1.5 irradiation from a solar simulator (Newport-Oriel 91160) calibrated with a Si-based reference cell (Hamamatsu S1133) containing an IR-cut filter (KG5) to correct the spectral mismatch of the lamp.[24] The NT-DSSC devices were operated with illumination on the back side and the transparent counter electrode masked with a black plastic tape of the same size with a round hole to allow the actively illuminated area, 0.28 cm^2, for all measurements.[25]

The incident monochromatic photon-to-current conversion efficiency (IPCE) measurements were carried out with a home-built system, which includes a Xe lamp (PTi A-1010, 150 W), a monochromator (Dongwoo DM150i, 1200 gr/mm blazed at 500 nm), and a source meter (Keithley 2400, computer-controlled). A standard Si photodiode (ThorLabs FDS1010) was used as a reference to calibrate the power density of the light source at each wavelength so that the IPCE(λ) of the NT-DSSC device can be obtained according to the following equation

$$\mathrm{IPCE}(\lambda) = \mathrm{IPCE}_{\mathrm{ref}}(\lambda) \cdot \frac{J_{\mathrm{DSSC}}(\lambda)}{J_{\mathrm{ref}}(\lambda)} \quad (1)$$

where the $\mathrm{IPCE}_{\mathrm{ref}}(\lambda)$ of the Si photodiode is known from a calibration, and the current densities of the reference cell and the NT-DSSC device, $J_{\mathrm{ref}}(\lambda)$ and $J_{\mathrm{DSSC}}(\lambda)$, were measured under the same experimental conditions (excitation beam size ~0.08 cm^2).

3. Results and Discussion

3.1. Growing ATO Films with Various Lengths of NT Arrays. According to Grimes and co-workers,[14,17] the formation of ATO NT involves fluoride ions: the lengths of these tubes were proportional to the fluoride concentration and to the duration of anodization. We confirmed this correlation, but the tubes adhered more weakly to the substrate when the tubes grew longer. To discover optimal conditions for long tubes tightly grown on the substrate, we used NH_4F electrolyte in EG at four concentrations to anodize Ti foil with anodization for various durations. Figure 4 shows the variation of length of TiO_2 NT as a function of period of anodization (the corresponding SEM images of each datum showing the lengths of the tubes are given in the Supporting Information, Figures S1−S4); the length increased with increasing duration of anodization and F^-

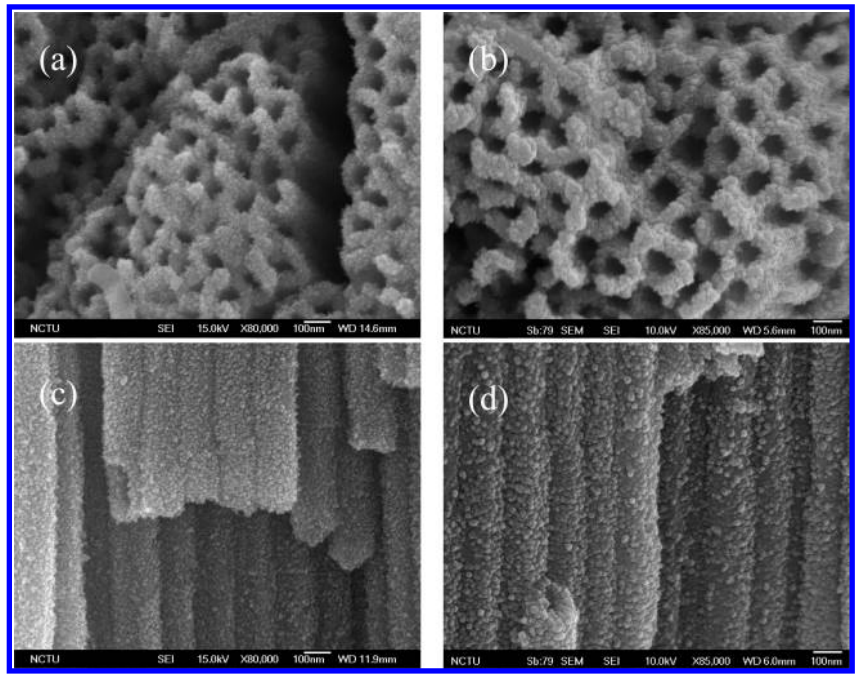

Figure 7. SEM images of ATO NT after treatments with $TiCl_4$: (a) and (c) top and side views with annealing temperature 350 °C; (b) and (d) top and side views with annealing temperature 450 °C. The scale bars represent a length of 100 nm.

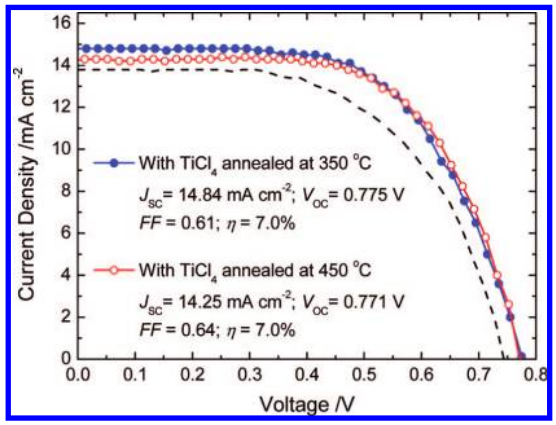

Figure 8. Current−voltage characteristics of NT-DSSC devices fabricated using the ATO films treated with $TiCl_4$ as shown in Figure 7 under simulated AM-1.5 solar illumination (100 mW cm^{-2}) and active area 0.28 cm^2. The dashed curve shows the results of an ATO film not treated with $TiCl_4$ for comparison.

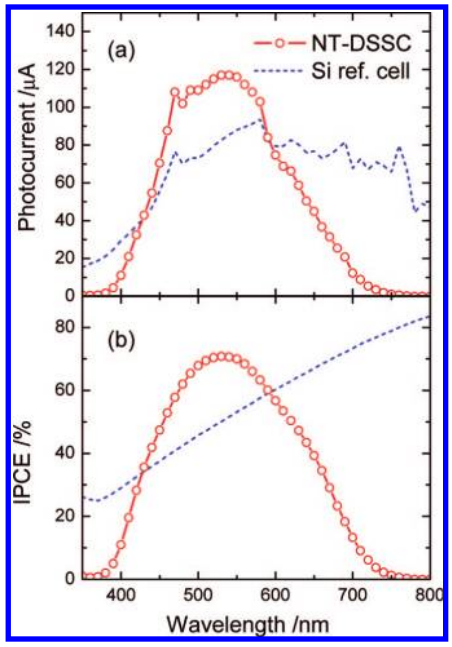

Figure 9. (a) Photocurrent and (b) IPCE spectra of the $TiCl_4$-treated NT-DSSC (circles) and the Si reference cell (dashed curves) measured at the same experimental conditions.

concentration. Our results indicate that the maximum lengths of NT with effective adhesion to the Ti substrate are 16, 20, 30, and 41 μm for NH_4F concentrations 0.15, 0.25, 0.5, and 0.8 wt % in EG, respectively. At small [F^-], the cracking was not severe, but the rate of tube growth was so small as to lead to formation of heavier clumps on the surface of the films. At large [F^-], even though the rate of tube growth was much increased, cracking also became significant, which causes poorer adhesion of the tubes to the substrate. As a compromise, we used ATO films grown with [NH_4F] at 0.5 wt % for various periods of anodization to investigate the dependence of the photovoltaic performance of NT-DSSC devices on length.

3.2. Photovoltaic Performance of the Devices with NT Arrays of Varied Lengths. The ability of the N3 dye chemisorbed on ATO films was examined with absorption spectra as shown in Figure 5a, in which the absorbance of the dye increases upon L increasing from 6 to 18 μm but varies insignificantly for L above 18 μm because of the saturation of the instrument (Supporting Information, Figure S5). The absorption maximum of the dye shifts slightly from 530 nm for shorter

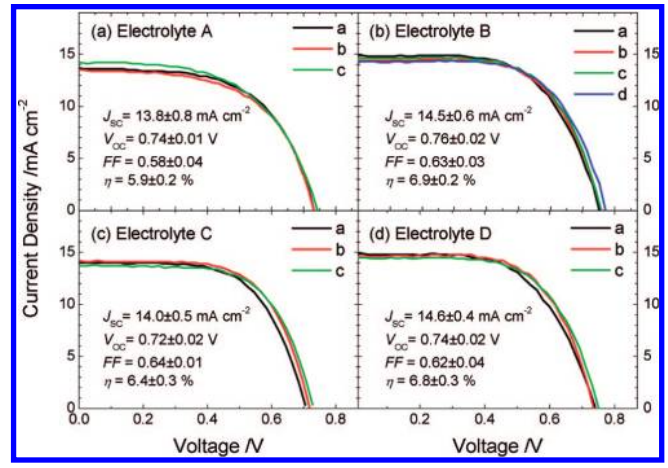

Figure 10. Current−voltage characteristics of NT-DSSC devices fabricated using four electrolytes: (a) electrolyte A, (b) electrolyte B, (c) electrolyte C, and (d) electrolyte D under simulated AM-1.5 solar illumination (100 mW cm^{-2}) and active area 0.28 cm^2. Three to four independent measurements were conducted with the same ATO films. The compositions of the electrolytes are summarized in Table 2.

tubes to 536 nm for longer tubes, together with a broad shoulder extending to greater wavelengths for the longer tubes. This spectral feature of the increased dye loading in longer tubes might be due to a saturation effect and/or due to the increase of molecular interaction that results in the broader shoulder toward the red part of the visible spectra. These N3/ATO films were fabricated into NT-DSSC devices of which the corresponding *IV* curves are shown in Figure 5b. We show the measured photovoltaic parameters of these devices in Figure 6; the corresponding values are summarized in Table 1, which demonstrates that the current density at short circuit (J_{SC} in mA cm^{-2}), the voltage at open circuit (V_{OC} in V), the fill factor (FF), and the efficiency of power conversion ($\eta = J_{SC} \cdot V_{OC} \cdot FF/P_{in}$ with $P_{in} = 100$ mW cm^{-2}) vary with the tube length (L). The results display a notably systematic trend for J_{SC}, such that the current density increases significantly from $J_{SC} = 6.4$ mA cm^{-2} at $L = 6$ μm to $J_{SC} = 12.5$ mA cm^{-2} at $L = 30$ μm because longer tubes offer a larger surface area on which the dye molecules adsorb.

Our results also show a systematic trend with both V_{OC} and FF decreasing upon increasing tube length. Because the extent of the increase in J_{SC} was much greater than the extent of the decrease in V_{OC} and FF, the overall efficiency of conversion of photons to current exhibited a systematic increase from $\eta = 3.0\%$ at $L = 6$ μm to $\eta = 5.2\%$ at $L = 30$ μm. A negative dependence of cell performance on length in both V_{OC} and FF is unambiguously shown in Figure 6, indicating that charge recombination might be important at the interface between the electrode and the electrolyte.[26,27] The source of charge recombination might have been the cracking of the films (Figure 1b), which became more significant for films of tubes of increasing length. To remedy this problem, we further treated the ATO films with $TiCl_4$.[28,29]

3.3. Photovoltaic Performance on $TiCl_4$ Treatments of ATO Films. The effect of the $TiCl_4$ treatment on ATO films is reported to increase the amount of dye loading and hence to enhance the photocurrent of the device.[18] In particular, it has been shown that the $TiCl_4$ treatment in a front-illuminated NT-DSSC increases the roughness of the tube walls and thus improves the cell performance through an increased effective surface area for dye adsorption.[8,18,20] The dye-loading experiments have confirmed that the amount of adsorbed N3 dye on

TABLE 2: Photovoltaic Performance of NT-DSSC at Four Compositions of Electrolytes under AM-1.5 Illumination (Power 100 mW cm^{-2}) and Active Area 0.28 cm^{2}[a]

electrolytes[b]	LiI/M	I_2/M	BMII/M	TBP/M	J_{SC}/mA cm^{-2}	V_{OC}/V	FF	η/%
A	0	0.01	0.6	*c*	13.8 ± 0.8	0.74 ± 0.01	0.58 ± 0.04	5.9 ± 0.2
B	0.1	0.01	0.6	0.5	14.5 ± 0.6	0.76 ± 0.02	0.63 ± 0.03	6.9 ± 0.2
C	0	0.03	0.6	0.5	14.0 ± 0.5	0.72 ± 0.02	0.64 ± 0.01	6.4 ± 0.3
D	0.05	0.03	1.0	0.5	14.6 ± 0.4	0.74 ± 0.02	0.62 ± 0.04	6.8 ± 0.3

[a] All photovoltaic parameters were obtained from averaging three to four sets of the *IV* curves shown in Figure 10; the uncertainties represent two standard errors. [b] Additional component in electrolytes A−D contains guanidinium thiocyanate (GuNCS, 0.1 M) in a mixture of acetonitrile and valeronitrile (volume ratio 15/1 for A and B, and 85/15 for C and D). [c] Electrolyte A contains no 4-*tert*-butylpyridine (TBP) but contains N-methylbenzimidazole (MBI, 0.5 M).

a $TiCl_4$-treated ATO film is larger than that adsorbed on an untreated ATO film (Supporting Information, Figures S6 and S7). We further tested the effect of the $TiCl_4$ treatments in a back-illuminated NT-DSSC by varying the immersion temperatures and periods and the annealing temperatures. According to those tests, the best condition was to treat $TiCl_4$ twice at 50 °C; for the first treatment, the films were immersed in $TiCl_{4(aq)}$ (0.1 M, 1.5 h) followed by appropriate rinsing and drying (300 °C, 30 min); for the second treatment, the films were immersed in $TiCl_{4(aq)}$ (0.1 M, 1.5 h) again and then annealed at either 350 or 450 °C for 30 min. Parts a/c and b/d of Figure 7 show top and side views of SEM images of the $TiCl_4$-treated ATO films ($L = 19$ μm) at annealing temperatures 350 and 450 °C, respectively. The two-step treatments of the ATO films with $TiCl_4$ clearly formed compact TiO_2 nanoparticles on the inner and outer surfaces of the NT so as to increase the surface area for dye adsorption. The TiO_2 nanoparticles produced at an annealing temperature of 350 °C were smaller than those formed at 450 °C.

After the ATO films treated with $TiCl_4$ were sensitized with N3 dye, the N3/ATO films were fabricated into NT-DSSC together with an improved counter electrode.[30] The effect of $TiCl_4$ treatment on cell performance is shown in Figure 8; the *IV* characteristic of an ATO film not treated with $TiCl_4$ appears as a dashed curve ($J_{SC} = 13.8$ mA cm^{-2}; $V_{OC} = 0.741$ V; FF = 0.58; $\eta = 5.9\%$) for comparison. After posttreatment of the ATO films with $TiCl_4$, J_{SC}, V_{OC}, and FF of the NT-DSSC devices increased significantly, so improving the cell performance from $\eta = 5.9\%$ to $\eta = 7.0\%$. Both $TiCl_4$-treated ATO films have similar values of η. Although the values of V_{OC} are similar, the value of J_{SC} for the film annealed at 350 °C is greater than that for annealing at 450 °C owing to larger surface area of the former for enhanced dye loading. A higher temperature of annealing of the latter might aid nucleation of the nanoparticular TiO_2 into the anatase phase for improved electron transport and hence an increased fill factor of the device. These two effects appeared to balance each other, such that almost the same cell performance was obtained for the two-step $TiCl_4$ treatments at two annealing temperatures.

The photocurrent action (IPCE) spectrum of the $TiCl_4$-treated NT-DSSC device was obtained from a calibrated experiment. Figure 9a shows the photocurrents of NT-DSSC (circles) and the Si reference cell (dashed curve), which were obtained under the same experimental conditions. Because the $IPCE_{ref}(\lambda)$ of the reference cell was known (dashed curve in Figure 9b), the $IPCE(\lambda)$ of the NT-DSSC device can be evaluated according to eq 1, and the results are shown as circles in Figure 9b. The IPCE spectrum exhibits a maximum around 530 nm, which is similar to the feature of the absorption spectra of the N3/ATO films shown in Figure 5a. Furthermore, our IPCE spectrum is also similar to the IPCE spectrum of a back-illuminated NP-DSSC device with $\eta = 7.2\%$.[21] It was pointed out[21] that the IPCE values of a back-illuminated DSSC device are lower than those of its front-illuminated counterpart owing to the absorption of the I_3^- electrolyte that cuts the incident light significantly below 500 nm.

To save time in loading the dye onto the ATO films, we used the N3 dye with immersion period 8 h, whereas Grimes and co-workers[17] used N719 dye with immersion period 48 h, and this leads to a lower V_{OC} value being observed.[31] The duration of growth of an ATO film with $L = 20$ μm was much smaller in our case (3−4 vs 24 h), which might be an important concern for future commercialization of a NT-DSSC.

3.4. Effect of the Redox Electrolytes. Because sunlight is transmitted through the redox electrolyte before being absorbed by dye molecules in a back-illuminated NT-DSSC device, the composition of the electrolyte might play a role in the cell performance. For example, Grimes and co-workers reported $\eta = 5.44\%$ for their back-illuminated NT-DSSC result with the electrolyte solution composed of LiI (0.5 M), I_2 (0.05 M), TBP (0.5 M), N-methylbenzimidazole (MBI, 0.6 M), and GuNCS (0.1 M) in methoxypropionitrile (MPN); their device suffers from a small FF value (0.43), which was attributed to a thick barrier layer of the ATO film.[14] The large concentrations of LiI and I_2 in the electrolyte might obstruct significantly the incident light in a backside illumination device. The same group subsequently reported $\eta = 6.89\%$ for an electrolyte containing I_2 (0.01 M), MBI (0.5 M), BMII (0.6 M), and GuNCS (0.1 M) in MPN.[17] Our tests indicate that this electrolyte still suffers from a small FF value, probably due to the large viscosity of MPN; altering the MPN solvent to a cosolvent of acetonitrile and valeronitrile with a volume ratio 15:1 (electrolyte A in Table 2) much improves the cell performance ($\eta = 5.9\%$). TBP in the electrolyte is known to play an important role in increasing both V_{OC} and FF values through remedying the dye-uncovered surface of the ATO films.[28] Recent investigations[32,33] show that addition of TBP containing Li^+ ions in the electrolyte reduces the surface positive charge, which shifts the conduction band potential of TiO_2 toward negative and leads to the increase of V_{OC}. Furthermore, TBP suppressed the recombination between the injected electrons and triiodide anions that leads to the increase of V_{OC} and FF.[33,34] By replacement of the MBI component with TBP (0.5 M) and addition of LiI (0.1 M) to increase the iodine anions, the device made of electrolyte B produces much better cell performance than the device made of electrolyte A (Table 2).

The *IV* characteristics of the NT-DSSC made of four electrolytes (A−D), repeated three to four times, are shown in Figure 10; the corresponding averaged photovoltaic parameters are summarized in Table 2. Electrolyte C, adopted from Grätzel and co-workers,[21] was designed for both front- and back-illuminated NP-DSSC devices. The large concentration of I_2 and lack of Li^+ in electrolyte C lead to the decrease in both J_{SC} and V_{OC} that causes device C to have a deteriorated cell

performance relative to device B ($\eta = 6.4\%$ vs $\eta = 6.9\%$). Because the presence of Li^+ ions might increase the amount of TBP adsorption on TiO_2 surface,[32] lack of Li^+ ions in electrolyte C could result in lower V_{OC} as we have observed (Table 2). Increasing the concentration of I_2 increases the concentration of triiodide anions so increasing the hole transport mobility, but this effect is balanced in a back-illuminated device by the attenuation of the incident light in the visible region ($\lambda < 500$ nm). However, the cell performance improved significantly with the additions of 0.05 M LiI and 1.0 M BMII in electrolyte D, which is a new redox electrolyte for NP-DSSC reported by Grätzel and co-workers.[35] The performance of device D is comparable to that of device B, which gives the best cell performance for a back-illuminated NT-DSSC device.

4. Conclusion

In summary, we fabricated dye-sensitized solar cells based on working electrodes made of highly ordered anodic titanium oxide nanotube arrays of varied tube length directly formed on Ti foil. The lengths of these ATO NT were controlled from 4 to 41 μm while varying the concentrations of NH_4F electrolyte (0.1, 0.25, 0.5, and 0.8 wt %) in EG in the presence of H_2O (2 vol %) for various periods ($t = 0.5-8$ h) of anodization. The unwanted surface deposits introduced during anodization were effectively removed simply with ultrasonic cleaning. After sensitization of the ATO film with N3 dye, the N3/ATO film served as a working electrode to fabricate a NT-DSSC device. We observed a systematic variation of the photovoltaic performance of NT-DSSC devices (with NH_4F at 0.5 wt %) increasing from 3.0% to 5.2% as L was increased from 6 μm ($t = 0.5$ h) to 30 μm ($t = 8$ h). After posttreatment of ATO films with $TiCl_4$ by annealing in two steps, the cell performance of the NT-DSSC device increased further to $\eta = 7.0\%$ at $L = 19$ μm. The best electrolyte tested for a back-illuminated device contains LiI (0.1 M), I_2 (0.01 M), BMII (0.6 M), TBP (0.5 M), and GuNCS (0.1 M) in a mixture of acetonitrile and valeronitrile (v/v = 15/1). We emphasize the significance of the present work for the growth of ATO films with longer nanotubes at much smaller periods of anodization, which might be an important concern for future commercialization of NT-DSSC.

Acknowledgment. The National Science Council of the Republic of China provided financial support through project contracts 96-2628-M-009-018-MY2 and 96-2627-M-009-005. Support from the MOE-ATU program and Niching Industrial Corporation are also acknowledged.

Supporting Information Available: Side-view SEM images of the ATO films shown in Figure 4, absorption spectra of the N3/ATO films shown in Figure 5a, absorption spectra of dye-loading experiments, TEM images of Pt-sputtered patterns, and transmission spectra of Pt-sputtered FTO substrates. This information is available free of charge via the Internet at http://pubs.acs.org.

References and Notes

(1) O'Regan, B.; Grätzel, M. *Nature* **1991**, *353*, 737.

(2) Nazeeruddin, M. K.; Angelis, F. D.; Fantacci, S.; Selloni, A.; Viscardi, G.; Liska, P.; Ito, S.; Takeru, B.; Grätzel, M. *J. Am. Chem. Soc.* **2005**, *127*, 16835.

(3) Wang, Q.; Ito, S.; Grätzel, M.; Fabregat-Santiago, F.; Mora-Seró, I.; Bisquert, J.; Bessho, T.; Imai, H. *J. Phys. Chem. B* **2006**, *110*, 25210.

(4) Wei, M.; Konishi, Y.; Zhou, H.; Yanagida, M.; Sugihara, H.; Arakawa, H. *J. Mater. Chem.* **2006**, *16*, 1287.

(5) Koide, N.; Islam, A.; Chiba, Y.; Han, L. *J. Photochem. Photobiol., A* **2006**, *182*, 296.

(6) Chiba, Y.; Islam, A.; Watanabe, Y.; Komiya, R.; Koide, N.; Han, L. *Jpn. J. Appl. Phys* **2006**, *45*, L638.

(7) Law, M.; Greene, L. E.; Johnson, J. C.; Saykally, R.; Yang, P. *Nat. Mater.* **2005**, *4*, 455.

(8) Mor, G. K.; Shankar, K.; Paulose, M.; Varghese, O. K.; Grimes, C. A. *Nano Lett.* **2006**, *6*, 215.

(9) Song, M. Y.; Kim, D. K.; Ihn, K. J.; Jo, S. M.; Kim, D. Y. *Nanotechnology* **2004**, *15*, 1861.

(10) Cheung, K. Y.; Yip, C. T.; Djurišić, A. B.; Leung, Y. H.; Chan, W. K. *Adv. Funct. Mater.* **2007**, *17*, 555.

(11) Peng, T.; Hasegawa, A.; Qiu, J.; Hirao, K. *Chem. Mater.* **2003**, *15*, 2011.

(12) Adachi, M.; Murata, Y.; Okada, I.; Yoshikawa, S. *J. Electrochem. Soc.* **2003**, *150*, G488.

(13) Ngamsinlapasathian, S.; Sakulkhaemaruethai, S.; Pavasupree, S.; Kitiyanan, A.; Sreethawong, T.; Suzuki, Y.; Yoshikawa, S. *J. Photochem. Photobiol., A* **2004**, *164*, 145.

(14) Mor, G. K.; Varghese, O. K.; Paulose, M.; Shankar, K.; Grimes, C. A. *Solar Energy Mater. Solar Cells* **2006**, *90*, 2011. and related references therein.

(15) Wang, H.; Yip, C. T.; Cheung, K. Y.; Djurišić, A. B.; Xie, M. H.; Leung, Y. H.; Chan, W. K. *Appl. Phys. Lett.* **2006**, *89*, 023508.

(16) Zhu, K.; Neale, N. R.; Miedaner, A.; Frank, A. J. *Nano Lett.* **2007**, *7*, 69.

(17) Shankar, K.; Mor, G. K.; Prakasam, H. E.; Yoriya, S.; Paulose, M.; Varghese, O. K.; Grimes, C. A. *Nanotechnology* **2007**, *18*, 065707.

(18) Shankar, K.; Bandara, J.; Paulose, M.; Weitasch, H.; Varghese, O. K.; Mor, G. K.; LaTempa, T. J.; Thelakkat, M.; Grimes, C. A. *Nano Lett.* **2008**, *8*, 1654.

(19) Kuang, D.; Brillet, J.; Chen, P.; Takata, M.; Uchida, S.; Miura, H.; Sumioka, K.; Zakeeruddin, S. M.; Grätzel, M. *ACS Nano.* **2008**, *2*, 1113.

(20) Park, J. H.; Lee, T.-W.; Kang, M. G. *Chem. Commun.* **2008**, 2867.

(21) Ito, S.; Ha, M. C.; Rothenberger, G.; Liska, P.; Comte, P.; Zakeeruddin, S. M.; Péchy, P.; Nazeeruddin, M. K.; Grätzel, M. *Chem. Commun.* **2006**, 4004.

(22) Zhu, K.; Vinzant, T. B.; Neale, N. R.; Miedaner, A.; Frank, A. J. *Nano Lett.* **2007**, *7*, 3739.

(23) Paulose, M.; Shankar, K.; Yoriya, S.; Prakasam, H. E.; Varghese, O. K.; Mor, G. K.; Latempa, T. A.; Fitzgerald, A.; Grimes, C. A. *J. Phys. Chem. B* **2006**, *110*, 16179.

(24) Ito, S.; Matsui, H.; Okada, K.; Kusano, S.; Kitamura, T.; Wada, Y.; Yanagida, S. *Sol. Energy Mater. Sol. Cells* **2004**, *82*, 421.

(25) Ito, S.; Nazeeruddin, M. K.; Liska, P.; Comte, P.; Charvet, R.; Péchy, P.; Jirousek, M.; Kay, A.; Zakeeruddin, S. M.; Grätzel, M. *Prog. Photovolt.: Res. Appl.* **2006**, *14*, 589.

(26) Ito, S.; Liska, P.; Comte, P.; Charvet, R.; Péchy, P.; Bach, U.; Schmidt-Mende, L.; Zakeeruddin, S. M.; Kay, A.; Nazeeruddin, M. K.; Grätzel, M. *Chem. Commun.* **2005**, 4351.

(27) Bandaranayake, K. M. P.; Senevirathna, M. K. I.; Weligamuwa, P. M. G. M. P.; Tennakone, K. *Coord. Chem. Rev.* **2004**, *248*, 1277.

(28) Nazeeruddin, M. K.; Kay, A.; Rodicio, I.; Humphry-Baker, R.; Müller, E.; Liska, P.; Vlachopoulos, N.; Grätzel, M. *J. Am. Chem. Soc.* **1993**, *115*, 6382.

(29) Barbé, C. J.; Arendse, F.; Comte, P.; Jirousek, M.; Lenzmann, F.; Shklover, V.; Grätzel, M. *J. Am. Ceram. Soc.* **1997**, *80*, 3157.

(30) Because the performance of a back-illuminated NT-DSSC is very sensitive to the quality of the counter electrode, we tested the cell performance with the electrode made of highly transparent FTO glass sputtered by a thin layer of platinum. We found that the active area (0.28 cm^2) of the counter electrode of Pt sputtered for 14 s (power 10 W; target size 81 cm^2; distance from the target 15 cm; deposition rate 10 nm min^{-1}) would give the best result (the corresponding TEM images and transmission spectra are given in the Supporting Information as Figures S8 and S9, respectively). Furthermore, masking the rest of the active area by sputtering Pt for 10 min increases the electric conductivity of the counter electrode, which improves the cell performance significantly (Supporting Information Figure S10).

(31) The N3 dye has a higher extinction coefficient than does N719 so that the J_{SC} of the DSSC made of N3 is larger than that made of N719. However, N719 contains ammonium cations to remedy the TiO_2 surface so to obtain a larger V_{OC} than N3. Refer to, e.g., Horiuchi, T.; Miura, H.; Sumioka, K.; Uchida, S. *J. Am. Chem. Soc.* **2004**, *126*, 12218.

(32) Nakade, S.; Kanzaki, T.; Kubo, W.; Kitamura, T.; Wada, Y.; Yanagida, S. *J. Phys. Chem. B* **2005**, *109*, 3480.

(33) Boschloo, G.; Häggman, L.; Hagfeldt, A. *J. Phys. Chem. B* **2006**, *110*, 13144.

(34) Hara, K.; Dan-oh, Y.; Kasada, C.; Ohga, Y.; Shinpo, A.; Suga, S.; Sayama, K.; Arakawa, H. *Langmuir* **2004**, *20*, 4205.

(35) Gao, F.; Wang, Y.; Zhang, J.; Shi, D.; Wang, M.; Humphry-Baker, R.; Wang, P.; Zakeeruddin, S. M.; Grätzel, M. *Chem. Commun.* **2008**, 2635.

JP806281R